Int. J. Electrochem. Sci., 11 **(2016)** 1135 - 1151

International Journal of
ELECTROCHEMICAL
SCIENCE
www.electrochemsci.org

Aryl Aminoalcohols as Corrosion Inhibitors for Carbon Steel in Chloride-Contaminated Simulated Concrete Pore Solution

J. Z. Liu[1], *D. Zhao*[1,*], *J. S. Cai*[1], *L. Shi*[1], *J. P. Liu*[1,2]

[1] State Key Laboratory of High Performance Civil Engineering Materials, Jiangsu Research Institute of Building Science, Nanjing 211103 (P. R. China)
[2] Jiangsu Key Laboratory of Construction Materials, College of Materials Science and Engineering, Southeast University, Nanjing 211189 (P. R. China)
[*]E-mail: zhaodan@cnjsjk.cn

Received: 24 November 2015 / *Accepted:* 14 November 2015 / *Published:* 1 January 2016

In this paper, the rarely studied aryl aminoalcohols, namely comp. a-c were synthesized and then their corrosion inhibitions for carbon steel in 0.3 M NaCl saturated $Ca(OH)_2$ solutions were investigated using electrochemical techniques. The potentiodynamic polarization and electrochemical impedance spectroscopy tests showed comp. a and c had higher corrosion inhibition efficiencies than the most commonly used aminoalcohol type inhibitor *N*,*N*-dimethylaminoethanol (DMEA), but comp. b seemed no suppression of corrosion process. Based on the obtained results and previous work, we made a brief discussion on the inhibitive effectiveness related to the N-substituents of tested organic compounds. Besides, comp. a with the highest inhibition efficiency was further investigated, and it could act as an anodic inhibitor by a comprehensive interaction with the carbon steel surface according to the Langmuir adsorption isotherm. The surface morphology of the carbon steel observed by scanning electron microscope showed a less amount of corrosion pits formed under inhibited conditions.

Keywords: carbon steel; corrosion inhibitor; aminoalcohol; simulated concrete pore solution; adsorption

1. INTRODUCTION

It is well known that reinforced concrete is one of most widely used building materials in infrastructures such as buildings and bridges. Steel embedded in concrete normally remains stable because of a passive film formed during the cement hydration process.[1,2] However, when the passive film is destroyed by the presence of chlorides, corrosion of the reinforcing steel is initiated.[3,4] Over the past decades, many available techniques had been developed to prevent or at least reduce

corrosion of steel in concrete,[2,5] among which application of corrosion inhibitors was a more attractive one for its low cost and easy handling.[6−8]

Generally, corrosion inhibitors can be classified as inorganic or organic substances.[9−20] As typical inorganic inhibitors, nitrites protect the steel via oxidizing ferric ions to form a ferric-oxide film, which means re-construction of the passive film.[9] In contrast, most of the organic inhibitors absorb on metal surfaces via heteroatoms such as nitrogen, sulfur, oxygen, phosphorus and multiple bonds or aromatic rings, subsequently blocking the active sites and decreasing the corrosion rates.[16,21−24] Thus, many organic substances which have the ability to form an absorbed film on the steel surfaces could be treated as potential corrosion inhibitors if ignoring their influence on concrete properties such as strength, setting time, workability and durability.

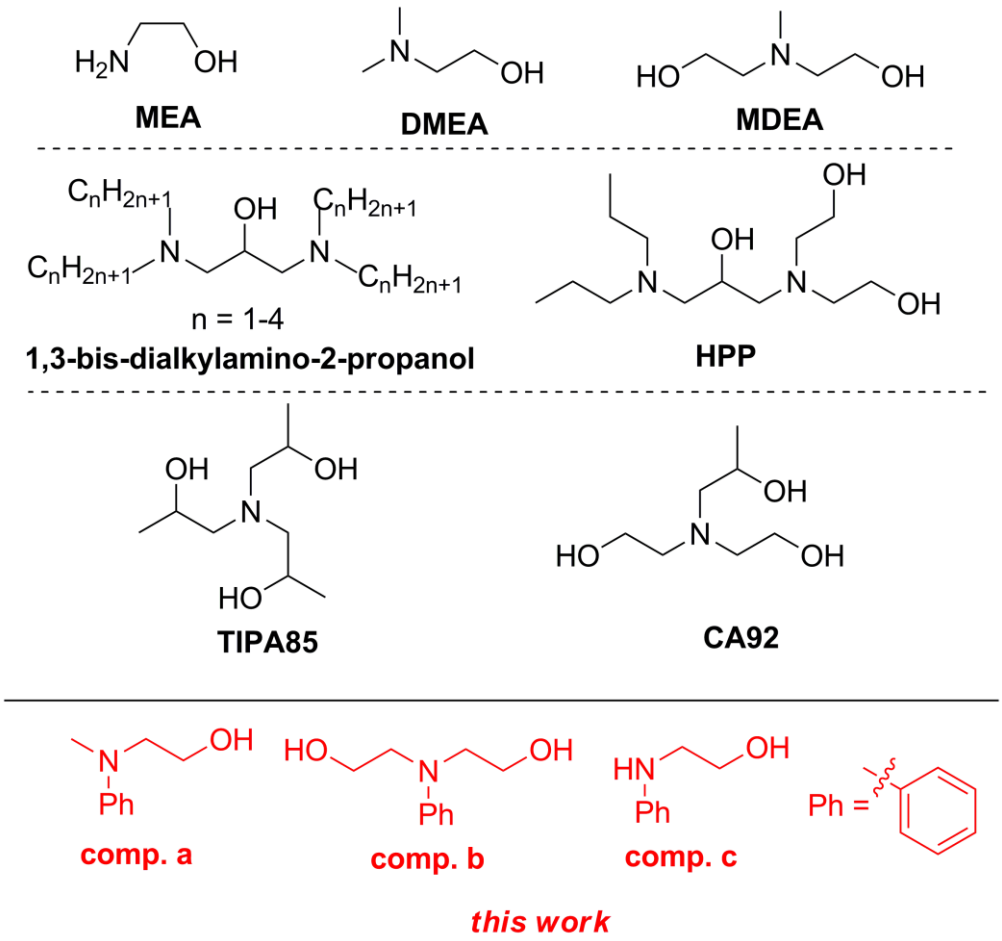

Figure 1. Molecular structures of aminoalcohol type inhibitors

Among these substances, amino alcohols were widely used as components in commercial products due in part to their attractive cost and less detrimental effect on concrete.[25,26] Besides, amino alcohol based corrosion inhibitors could be used either as concrete admixtures or to repair the existing structures.[27] For example, DMEA (Fig. 1) was the main active component of an organic surface-applied corrosion inhibitor and was experimentally investigated both in solution and concrete.[28,29] Recent studies indicated that the addition of DMEA to the simulated concrete pore

(SCP) solution as well as into the concrete contaminated with chloride ions decreased the corrosion rate of steel reinforcement.[30] The same opinion on corrosion efficiency was given by Xu, however, the author also pointed out DMEA exerted obvious influence on the chloride threshold level for corrosion of steel neither in the solution nor in the chloride contaminated concrete.[31]

According to previous reports, DMEA derivatives could serve as efficient catalysts to promote direct C-H arylation through the formation of five-membered chelate ring with the alkali metal ion.[32] Similarly, it was expected that DMEA coordinated to iron center followed by the formation of absorbed film to resist chloride attack. In this respect, the apposite electronic property and steric effect of the substituent linked to nitrogen atom contributed to form a more stable film on the steel surfaces. In 2009, Ormellese made basic investigations on the inhibitive action of several amino alcohol molecules, such as 2-aminoethanol (MEA), DMEA and 2,2'-(methylazanediyl)diethanol (MDEA) (Fig. 1), through electrochemical potentiodynamic polarization tests in SCP solutions.[33] In presence of 0.3 M chlorides, pitting potential of MEA was higher than that of DMEA, indicating a better inhibitive effectiveness. Notably, for MDEA with two hydroxyl groups, decrease of pitting potential compared with SCP solution containing 0.3 M chlorides was observed, revealing negative effect. In 2012, our group reported the inhibitive behaviors of 1,3-bis-dialkylamino-2-propanol derivatives (Fig. 1) and the results showed that a longer alkyl chain afforded a higher inhibition efficiency.[34,35] Later on, to increase the solubility as well as adsorption ability, we prepared a novel amino alcohol 2,2'-((3-(dipropylamino)-2-hydroxypropyl)azanediyl)diethanol (HPP) (Fig. 1) with more hydroxyl, amino groups and proper long alkyl chains.[36] Very recently, cement grinding aid alcamines, such as 1,1',1''-nitrilotris(propan-2-ol) (TIPA85) and 2,2'-((2-hydroxypropyl)azanediyl)diethanol (CA92) (Fig. 1) were studied as corrosion inhibitors for reinforced steel and a clearly beneficial steric effect was observed.[37]

Despite pioneering work achieved in this field, the study of structure-activity relationship seemed superficial.[33,38] Besides, amino alcohol type corrosion inhibitors were limited to N-alkyl substituted ones, which the inhibitive effectiveness was mainly dependent on steric and hydrophobic effects rather than the electronic properties of the substituents considering the electron-donating ability of alkyl groups were weak and the inductive effect weakened rapidly over a short distance along the carbon chain.[39] On the other hand, aromatic rings were voluminous and the electron-rich π system would be responsible for electrostatic repulsion towards chlorides. Besides, the electron density in nitrogen atom which was governed by inductive and p-π conjugate effects between amino group and aromatic ring would partly influenced the absorption of corrosion inhibitors on steel surfaces.[33] Thus, the inhibition mechanism of aryl aminoalcohol was theoretically different from alkyl aminoalcohol.

Encouraged by the above reports, and in continuation of our research on structure-activity relationship, we herein synthesize three aryl aminoalcohols 2-(methyl(phenyl)amino)ethanol (comp. a), 2,2'-(phenylazanediyl)diethanol (comp. b) and 2-(phenylamino)ethanol (comp. c) (Fig. 1), and we also make fundamental evaluations of these compounds. To the best of our knowledge, this is the first example of aryl aminoalcohols applied as corrosion inhibitors. The objective of this work is to study the role of substituents, especially the aryl group on inhibition effectiveness in chloride contaminated

SCP solutions. The electrochemical performance of carbon steel electrode was investigated by potentialdynamic polarization and electrochemical impedance spectroscopy (EIS) methods.

2. EXPERIMENTAL

2.1 Synthesis of aryl aminoalcohols

Unless otherwise indicated, all compounds and reagents were purchased from commercial suppliers and used without further purification. ^{1}H NMR was recorded on a Bruker AVANCE III 400 MHz spectrometer. Spin multiplicities are given as s (singlet), d (doublet), t (triplet) and q (quartet). Coupling constants (*J*) are given in hertz (Hz). ESI-MS was carried out on a LCMS-2020 (Shimadzu, Japan).

2-(methyl(phenyl)amino)ethanol (comp. a): To a DMF (50 mL) solution of N-methyl aniline (22 mL, 0.2 mol), K_2CO_3 (28 g, 0.2 mol) and KI (17g, 0.1 mol) was added 2-bromoethanol (16 mL, 0.22 mol) dropwise. The mixture was stirred at 90 °C for 24 h before cooled to RT. After the precipitate was removed by filtration, the organic phase was diluted with ethyl acetate and washed successively with water and brine, then dried over anhydrous Na_2SO_4. The solvent was removed under reduced pressure and then purified by flash column chromatography on silica gel to afford the desired product as brown oil.^{1}H NMR (400 MHz, DMSO-d_6) δ 7.14 (dd, *J* = 8.8, 7.2 Hz, 2H), 6.67 (d, *J* = 8.0 Hz, 2H), 6.58 (t, *J* = 7.2 Hz, 1H), 4.66 (t, *J* = 5.4 Hz, 1H), 3.54 (dd, *J* = 12.0, 6.2 Hz, 2H), 3.37 (dd, *J* = 7.5, 5.2 Hz, 2H), 2.90 (s, 3H).

N-phenyldiethanolamine (comp. b): To a H_2O (50 mL) suspension of aniline (18 mL, 0.2 mol), $CaCO_3$ (40 g, 0.4 mol) and KI (3.3g, 0.02 mol) was added 2-bromoethanol (36 mL, 0.5 mol) dropwise. The mixture was stirred at reflux for 12 h before cooled to RT. After the precipitate was removed by filtration, the suspension was extracted with ethyl acetate and the organic phase was washed with brine, and then dried over anhydrous Na_2SO_4. The solvent was removed under reduced pressure and then purified by flash column chromatography on silica gel to afford the desired product as white solid. ^{1}H NMR (400 MHz, DMSO-d_6) δ 7.12 (dd, *J* = 8.7, 7.3 Hz, 2H), 6.66 (d, *J* = 8.2 Hz, 2H), 6.54 (t, *J* = 7.2 Hz, 1H), 4.77 (t, *J* = 5.4 Hz, 2H), 3.54 (dd, *J* = 11.9, 6.2 Hz, 4H), 3.41 (t, *J* = 6.4 Hz, 4H).

2-(phenylamino)ethanol (comp. c):A mixture of aniline (28 mL, 0.3 mol) and 2-bromoethanol (14 mL, 0.2 mol) was heated at 90 °C under an argon atmosphere for 4 h. The resulting solid was dissolved in ethyl acetate, washed with 2 M aqueous NaOH followed by brine, and then the organic phase was dried over Na_2SO_4. Removal of the solvent under reduced pressure and then purified by flash column chromatography on silica gel to afford the desired product as yellow oil. ^{1}H NMR (400 MHz, DMSO-d_6) δ 7.06 (dd, *J* = 8.4, 7.3 Hz, 2H), 6.57 (d, *J* = 7.7 Hz, 2H), 6.51 (t, *J* = 7.2 Hz, 1H), 5.43 (t, *J* = 5.6 Hz, 1H), 4.69 (t, *J* = 5.5 Hz, 1H), 3.55 (q, *J* = 5.9 Hz, 2H), 3.08 (q, *J* = 6.0 Hz, 2H).

These spectral data indicated that the compounds were synthesized correctly with high purities (see copies of the ^{1}H NMR spectra in Supporting Information).

2.2 Materials and sample preparation

The test solution used in all experiments was saturated $Ca(OH)_2$ solution with 0.3 M NaCl prepared from reagent grade chemicals and bi-distilled water.

Working electrodes (Φ 8×5 mm) were cut from the carbon steel bar (Q235) with a composition (in mass%): C 0.17, Mn 0.46, Si 0.26, Cu 0.019, S 0.017, P 0.0047 and Fe balance. Before testing, the working electrodes were ground gradually with grit SiC paper (grade 240, 400, 1000 and 2000), then degreased and rinsed with ethanol.

2.3 Electrochemical measurements

The electrochemical measurements were performed in a conventional three-electrode cell with a volume of 0.3 L, equipped with Ag/AgCl electrode as the reference electrode, platinum mesh sheet as the counter electrode and exposed working area of working electrode was 0.36 cm^2. All the electrochemical experiments were carried out using P4000 (Princeton Applied Research). EIS was performed at the open circuit potential (OCP) in the frequency range of 100 kHz-10 mHz with a 10 mV amplitude signal after the electrodes were immersed in test solutions for 0.5h, using ZSimpWin software to fit the EIS data. The potentiodynamic measurements were done in the potential range from -200 to 800 mV versus the OCP with a scan rate of 0.5 mV/s after the electrodes were immersed in test solutions for 1.0h. All potentials reported in the paper were referred to Ag/AgCl electrode.

2.4 Surface analysis

The prepared working electrodes were immersed in 0.3 M NaCl SCP solutions in the absence (blank) and presence of 10 mM comp. a for 24 h, respectively. After removal from the test media, the electrodes were rinsed with deionised water and dried.The topographies of the steel surfaces were analyzed by SEM (JX A-8100,JEOL Co., Ltd) at an acceleration voltage of 15 kV.

3. RESULTS

3.1 Electrochemical measurements

3.1.1 Potentiodynamic polarization

Fig. 2 depicts polarization curves for carbon steel in 0.3 M NaCl SCP solutions in the absence (blank) and presence of comp. a. At 1 h immersion age, the corrosion potential moved positively with inhibitor concentration increased. Besides, the anodic process of carbon steel corrosion was effectively retarded by the inhibitor, and a higher concentration gave a lower corrosion current density. The results suggested that the addition of inhibitor reduced the anodic oxidation of iron and also retarded the oxygen reduction reaction which attributed to the formation of a more complete and stable barrier film on the steel surface.[40] Moreover, the increase of inhibitor concentration would result in a much more positive pitting potential and a wider passive region.

Table 1. The electrochemical parameters obtained from Fig. 2

Comp.	Conc. (mM)	E_{corr} (mv)	E_{pit} (mv)	E_{pit}-E_{corr} (mv)	$-\beta_c$ (mV dec^{-1})	β_a (mV dec^{-1})	I_{corr} (μA cm^{-2})	θ	IE (%)
blank	—	-435	—	—	287	506	17.2	—	—
comp. a	1	-407	—	—	123	131	4.23	0.754	75.4
	2	-358	-195	163	131	333	3.34	0.806	80.6
	5	-316	230	546	143	313	1.74	0.899	89.9
	10	-309	459	768	130	255	1.27	0.926	92.6

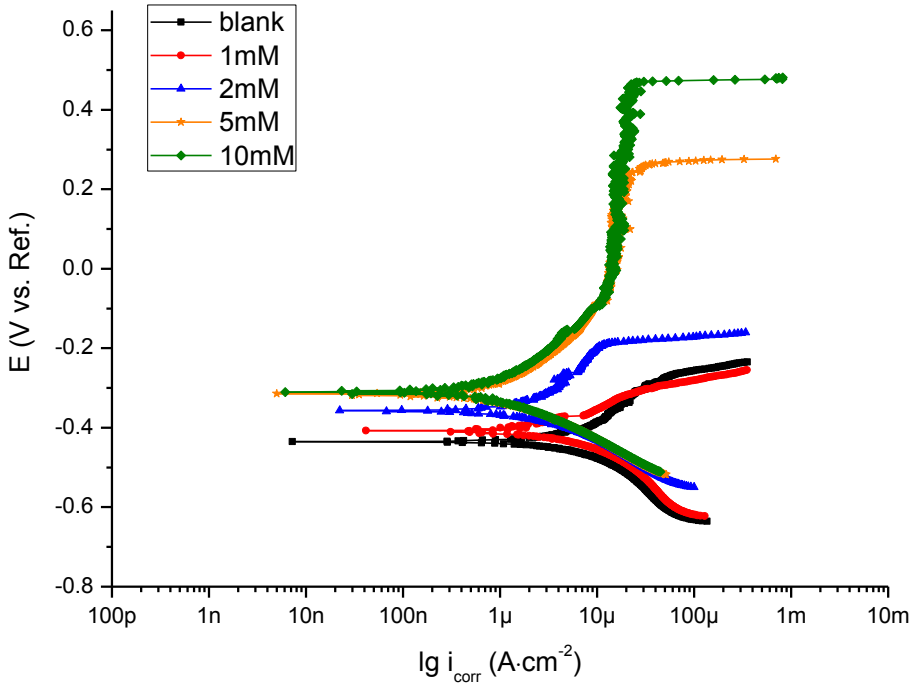

Figure 2. Potentiodynamic polarization curves for carbon steel in 0.3 M NaCl SCP solutions in the absence (blank) and presence of comp. a

Table 1 collects the fitted electrochemical parameters from polarization curves. E_{corr}, E_{pit} are corrosion potential and pitting potential, respectively. E_{pit}-E_{corr} is the width of the passive range, calculated from the difference between E_{pit} and E_{corr}. The cathodic (β_c) and anodic (β_a) slops are also obtained by fitting the polarization data in the vicinity of E_{corr} ±150 mV. The degree of surface coverage θ and inhibition efficiency IE are calculated by the following equations:

$$\theta = \frac{i^0_{corr} - i_{corr}}{i^0_{corr}} \quad (1)$$

$$IE = \frac{i^0_{corr} - i_{corr}}{i^0_{corr}} \times 100 \quad (2)$$

where i^0_{corr} and i_{corr} are the corrosion current densities of uninhibited and inhibited solutions, respectively. As shown in Table 1, the displacement of E_{corr} was larger than 85mV, indicating that comp. a was an anodic inhibitor.[41] When the concentration of comp. a was 10 mM, a satisfactory IE = 92.6% was measured.

Then, other aryl aminoalcohols as well as DMEA at the concentration of 10 mM were tested in 0.3 M NaCl SCP solutions through potentiodynamic polarization curves. The polarization curves and fitted electrochemical parameters are presented in Fig. 3 and Table 2, respectively.

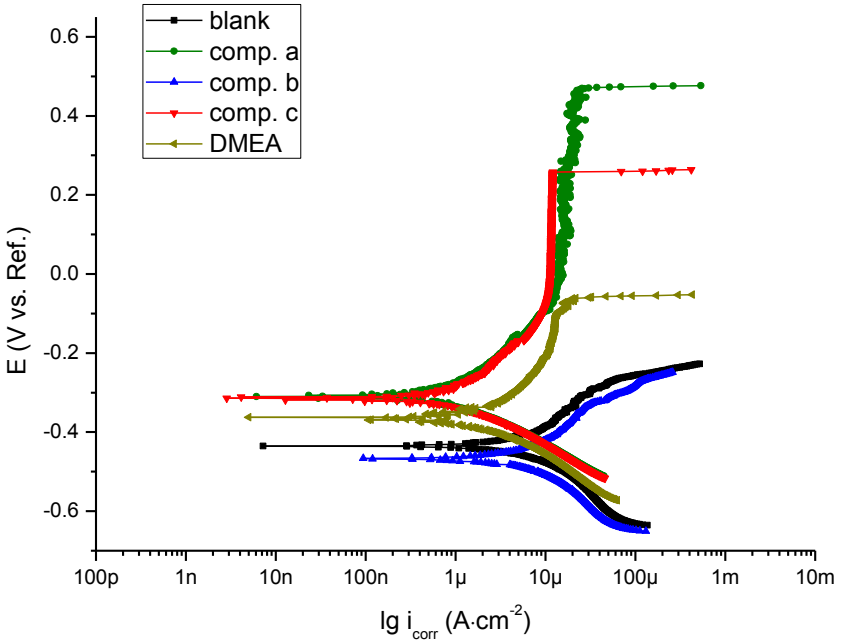

Figure 3. Potentiodynamic polarization curves for carbon steel in 0.3 M NaCl SCP solutions in the absence (blank) and presence of 10 mM different aminoalcohols

Among these inhibitors, comp. a showed the highest inhibition efficiency with the widest passive range, and comp. c also had a better inhibitive effectiveness than DMEA.

Table 2. The electrochemical parameters obtained from Fig. 3

Comp.	E_{corr} (mv)	E_{pit} (mv)	E_{pit}-E_{corr} (mv)	$-\beta_c$ (mV dec^{-1})	β_a (mV dec^{-1})	I_{corr} (μA cm^{-2})	IE (%)
blank	-435	—	—	287	506	17.2	—
comp. a	-309	459	768	130	255	1.27	92.6
comp. b	-467	—	—	364	525	20.5	—
comp. c	-315	247	562	138	288	1.54	91.0
DMEA	-366	-77	289	162	287	3.04	82.3

Confusingly, comp. b seemed no suppression of corrosion process, despite more hydroxyl groups existed in the molecule.

3.1.2 Electrochemical impedance

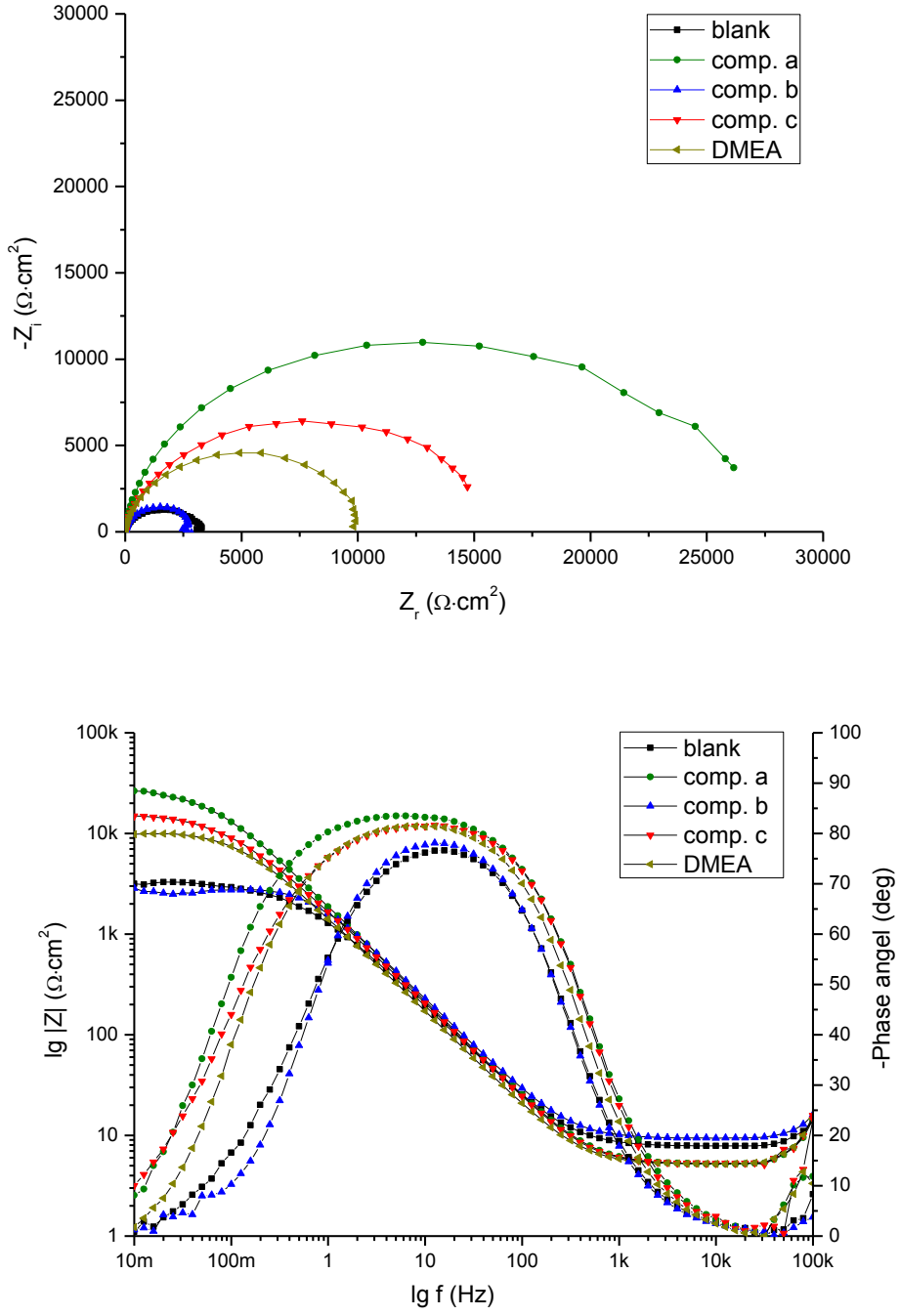

Figure 4. EIS Nyquist and Bode plots of the steel reinforcements immersed in 0.3 M NaCl SCP solutions in the absence (blank) and presence of 10 mM corrosion inhibitors

Fig. 4 depicts the EIS responses of the steel reinforcements immersed in 0.3 M NaCl SCP solutions in the absence and presence of 10 mM corrosion inhibitors. In comparison with the blank solution, the arc radiuses in Nyquist plots increased in the inhibited solutions except the solution containing comp. b. In Bode plots, impedance modulis in low frequency of the most inhibited systems

increased, indicating the corrosion was retarded by the aryl aminoalcohol type inhibitor due to the formation of a protective film on carbon steel surface.[42] In the presence of 10 mM comp. a, the reinforcing steel exhibited the maximum phase angle value of about 85°, while it was just about 75° without inhibitor.

Table 3. Fitted results from EIS for carbon steel in 0.3 M NaCl SCP solutions in the absence (blank) and presence of 10 mM different aminoalcohols

Comp.	R_s (Ω cm^2)	C_f (μF cm^{-2})	R_f (Ω cm^2)	C_{dl} (μF cm^{-2})	n	R_{ct} (kΩ cm^2)	IE (%)
blank	8.69	62.41	75.44	87.00	0.69	3.23	—
comp. a	6.70	63.16	346.50	32.20	0.80	25.63	87.4
comp. b	10.25	56.27	198.90	37.90	0.84	2.77	—
comp. c	7.03	66.41	353.50	57.27	0.69	16.08	79.9
DMEA	6.76	79.87	402.6	49.33	0.80	9.85	67.2

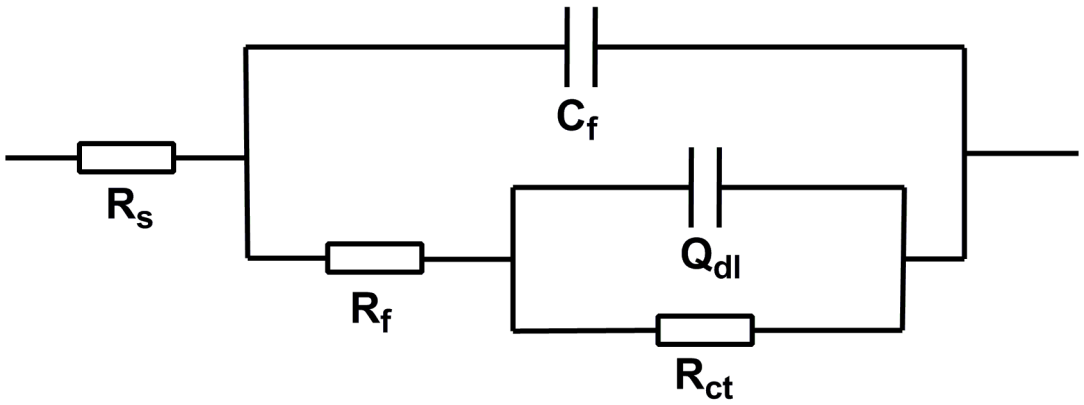

Figure 5. Electrochemical equivalent circuit

The experimental EIS response could be explained using an equivalent circuit, consisting of two time constants in series with the solution resistance, as shown in Fig. 5. Notably, this equivalent circuit was previously employed to simulate the aminoalcohol inhibited corrosion systems.[31,43] R_s represents the electrolyte resistance; R_f is the film resistance and R_{ct} represents the charge transfer resistance; C_f represents the film capacitance and CPE is the constant phase angle element to replace the double layer capacitance C_{dl}.The presence of the CPE is due to the distributed surface heterogeneity, roughness, fractal geometry, electrode porosity, and due to current and potential distributions related with electrode geometry. The associated impedance parameters are listed in Table 3, and the inhibition efficiency IE is calculated by the following equation:

$$IE = \frac{R_{ct} - R_{ct}^0}{R_{ct}} \times 100 \qquad (3)$$

where R_{ct}^0 and R_{ct} are the charge transfer resistances in uninhibited and inhibited systems, respectively. The comp. a inhibited system gave a higher R_{ct}, which was generally associated with a slower corrosion rate and a higher inhibition efficiency. The inhibition efficiencies of tested aminoalcohols were in good harmony with those obtained from potentiodynamic polarization. However, there was no clear regularity of the variation of R_f, probably because of the different molecular structures and adsorption performances on the steel surface. The inhibition efficiencies calculated through electrochemical measurements revealed that the order followed was: comp. a ＞ comp.c ＞ DMEA, and comp. b had no effect.

3.2 Adsorption isotherm

Adsorption isotherm was particularly important in understanding the interaction mechanism between organic corrosion inhibitors and steel surface.[44] In the present investigation, we found that the adsorption of the comp. a on the steel surface obeyed the Langmuir adsorption isotherm. According to Langmuir isotherm, the degree of surface coverage θ is related to inhibitor concentration C as:[45]

$$\frac{C}{\theta} = \frac{1}{K_{ads}} + C \qquad (4)$$

where K_{ads} is the adsorption equilibrium constant and the value of θ was listed in Table 1. The plot of C/h versus C yielded a straight line with a slope near to 1 and the correlation coefficient $R^2 = 0.999$, as shown in Fig. 6.

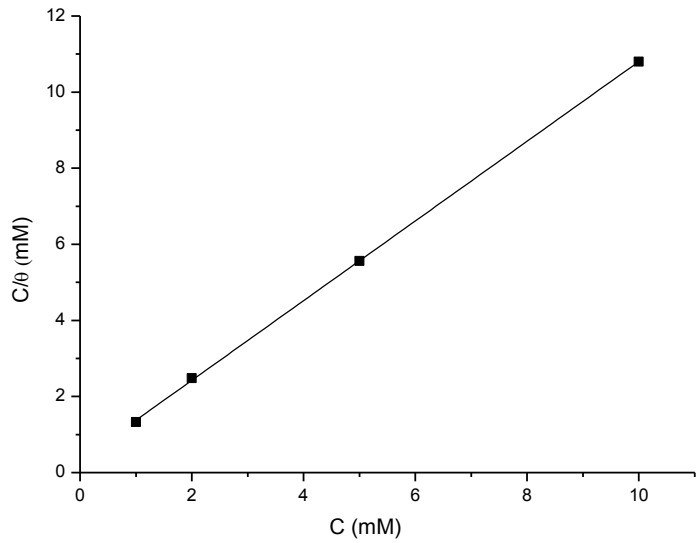

Figure 6. Langmuir adsorption isotherm of comp. a on carbon steel surface

Thus, the related standard free energy of adsorption ΔG_{ads}^0 can be estimated by the following equation:

$$\lg K_{ads} = \lg \frac{1}{55.5} - \frac{\Delta G_{ads}^0}{2.303RT} \qquad (5)$$

where the numeral of 55.5 is the molar concentration of water in solution, R is the universal gas constant, and T is the absolute temperature (298 K in this work). The calculated thermodynamic parameters are list in Table 4.

Table 4. Thermodynamic parameters for the adsorption of comp. a on carbon steel in 0.3 M NaCl SCP solutions

Comp.	slope	$K_{ads} \times 10^{-3}$ (L mol^{-1})	$-\Delta G^0_{ads}$ (kJ mol^{-1})	R^2
comp. a	1.05	3.04	29.8	0.999

Generally, the value of ΔG^0_{ads} up to -20 kJ mol^{-1} indicated a physical adsorption, while negative than -40kJ mol^{-1} involved sharing or transferring of electrons between the inhibitor molecule with the metal surface to form a coordinate type bond (chemical adsorption).[46] The calculated ΔG^0_{ads} value of comp. a was -29.8 kJ mol^{-1}, which accordingly showed a comprehensive adsorption on steel surface.

3.3 Surface analysis

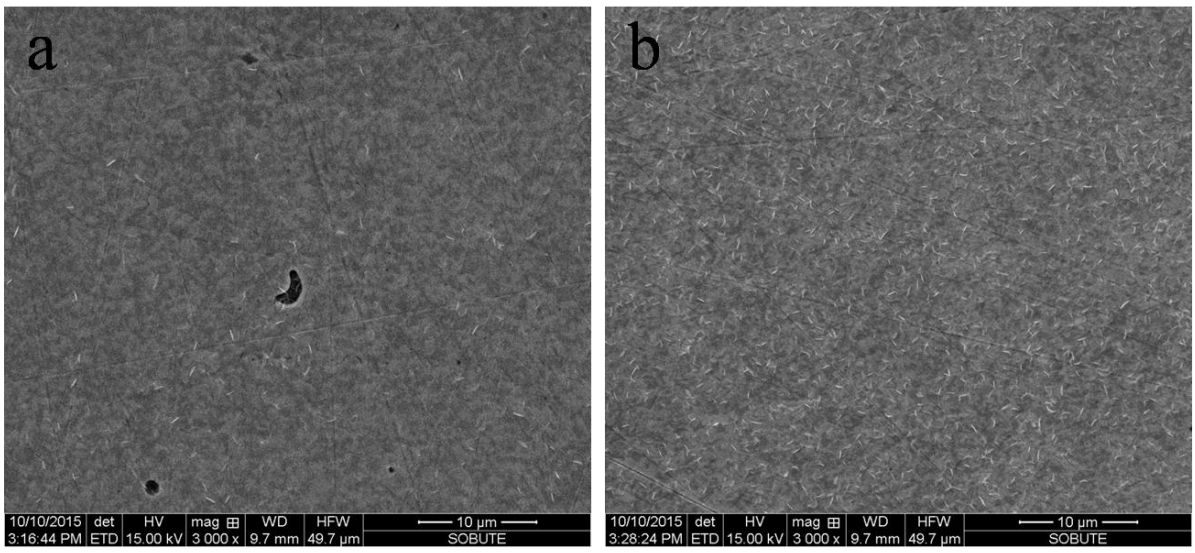

Figure 7. SEM micrographs (×3000) of carbon steel specimens immersed in 0.3 M NaCl SCP solutions (a) without and (b) with 10 mM comp. a for 24 h

Fig. 7 presents the SEM images of the steel surfaces immersed in 0.3 M NaCl SCP solutions in the absence (blank) and presence of 10 mM comp. a for 24 h, respectively. Obviously, there were significant differences between the specimens immersed in the test media without and with the inhibitor. Some small corrosion pits were observed on the surface of the reference sample, indicating a severe corrosion damage of the steel reinforcement. While in the inhibited conditions, corrosion pits disappeared, indicating comp. a exhibited an effective corrosion inhibition effect on the reinforcing steel. The above observations were consistent with the results from the electrochemical measurements.

4. DISCUSSION

To analyse separately the influence of substitutes in tested molecules on their inhibition efficiencies, firstly, we compared comp. a with DMEA. Phenyl was more voluminous than methyl group, forming a more efficient physical barrier that blocked or delayed chlorides arrival to the metal surface. Besides, the electron-rich π system developed a repulsive action towards chlorides, thereby inhibiting the iron dissolving process. Thus, both steric hindrance and electronic properties of phenyl group would contribute to a better inhibitive behavior than that of alkyl group.

Secondly, inhibition efficiency decreased when methyl was replaced by hydrogen (comp. a vs. comp. c), probably because of the intermolecular hydrogen bond interaction between amino group and water (N−H···O). In this interaction system, the amino group in comp. c acted as hydrogen bond donor, resulting in low electron density of nitrogen atom which decreased the absorption ability on steel surface.

Thirdly, for comp. b, a strange behavior was noticed: the additional hydroxyl group in the molecule had an adverse effect on corrosion inhibition. In previous report, MDEA (Fig. 1) which also belonged to N-substituted diethanolamine derivatives gave negative results compared with uninhibited solutions, suggesting this kind of compounds might present in the testing solutions at low concentrations due to their coordination interactions with Ca^{2+} in SCP solutions. To verify this hypothesis, some control experiments have been performed. It was reported that when ethanolamine coordinated with a metal ion, the resonance signals of group $–NCH_2$ shifted downfield obviously in the ^1H NMR spectra.[47] Accordingly, 10 mg comp. b was dissolved in D_2O in the absence and presence of $Ca(OH)_2$, respectively, and the ^1H NMR spectra were recorded (see Supporting Information). However, no changes of chemical shifts were detected, indicating there was no interaction between comp. b and Ca^{2+}. Besides, we also have not detected molecular-ion peaks of any potential comp. b-Ca^{2+} complexes in the mass spectra (see Supporting Information). Thus, the negative inhibition effectiveness of comp. b was most likely due to its weak interaction with iron, not due to 'precipitation' via coordinating with Ca^{2+}.

5. CONCLUSIONS

In summary, the corrosion performances of three aryl aminoalcohol type inhibitors have been evaluated in this study. The experiments were carried out in chloride contaminated SCP solutions using electrochemical techniques as well as surface analysis. In addition, ^1H NMR and mass spectrums were applied in the discussion of compound's structure on inhibitive behavior. Based on the experimental data, the following conclusion can be drawn:

(1) Comp. a acted as an anodic inhibitor, and with the increasing concentration that ranged from 1 to 10 mM, the inhibition effect improved gradually.

(2) The adsorption of comp. a corresponded well with Langmuir isotherm. The standard adsorption free energy was -29.8 kJ mol^{-1} in SCP solution with 0.3 M NaCl.

(3) The surface analysis verified that the adsorption of inhibitor comp. a on steel surface could effectively suppress the pitting corrosion induced by chloride.

(4) Aryl aminoalcohol inhibitors, especially comp. a showed better inhibition effectiveness than that of DMEA which was a common used component in the organic surface-applied corrosion inhibitor, probably because of the strong repulsive action towards chloride ions owing to both steric hindrance and electronic properties of phenyl group.

(5) According to basic adsorption mechanism, the inhibitive behavior of comp . b made us feel confused. Thus, the relationship between the molecular structures and the corrosion inhibitive mechanisms of amino alcohols still need to be further studied, and a standard method to predict the inhibition effectiveness of candidate inhibitors is highly desired.

SUPPORTING INFORMATION:

Spectral copies of ^{1}H NMR of comp. a-c

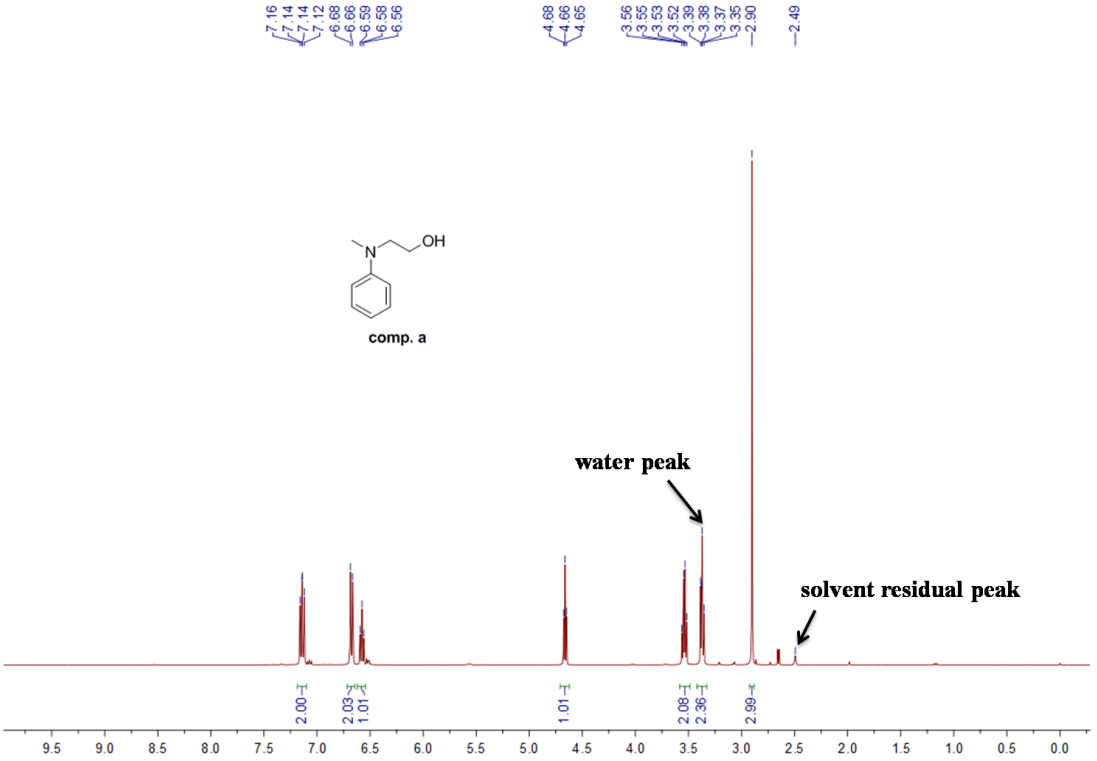

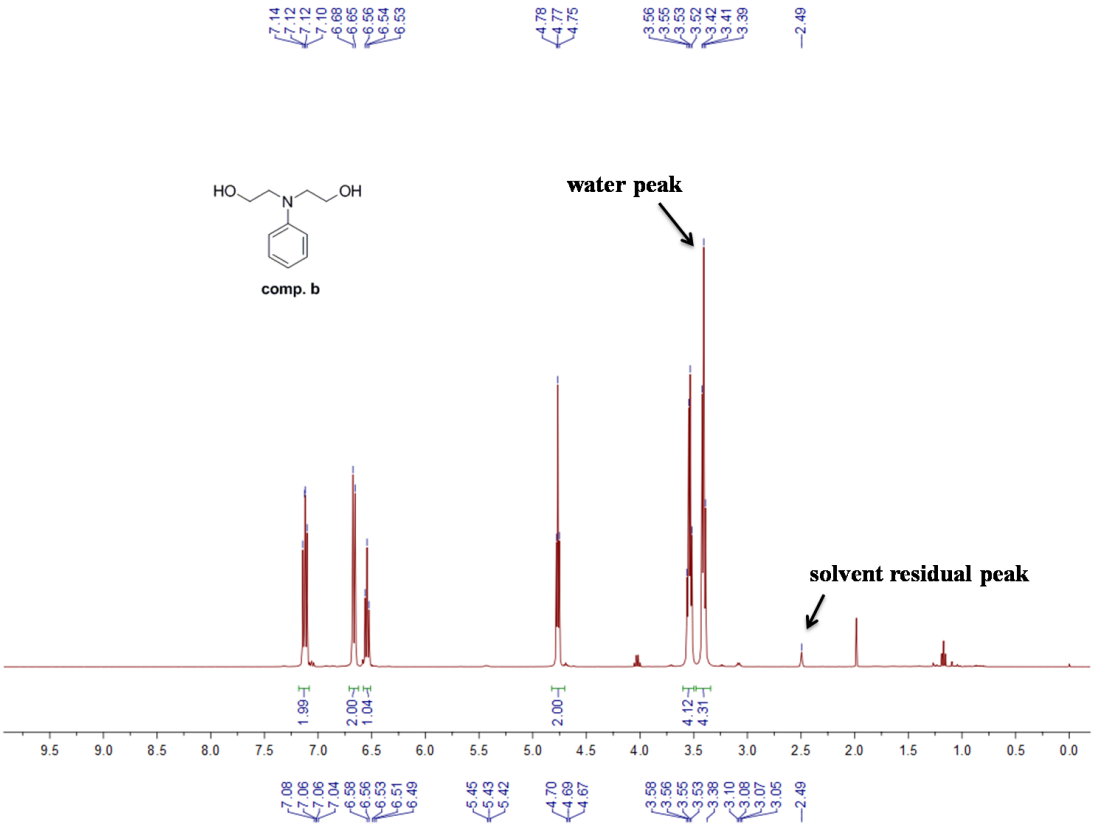

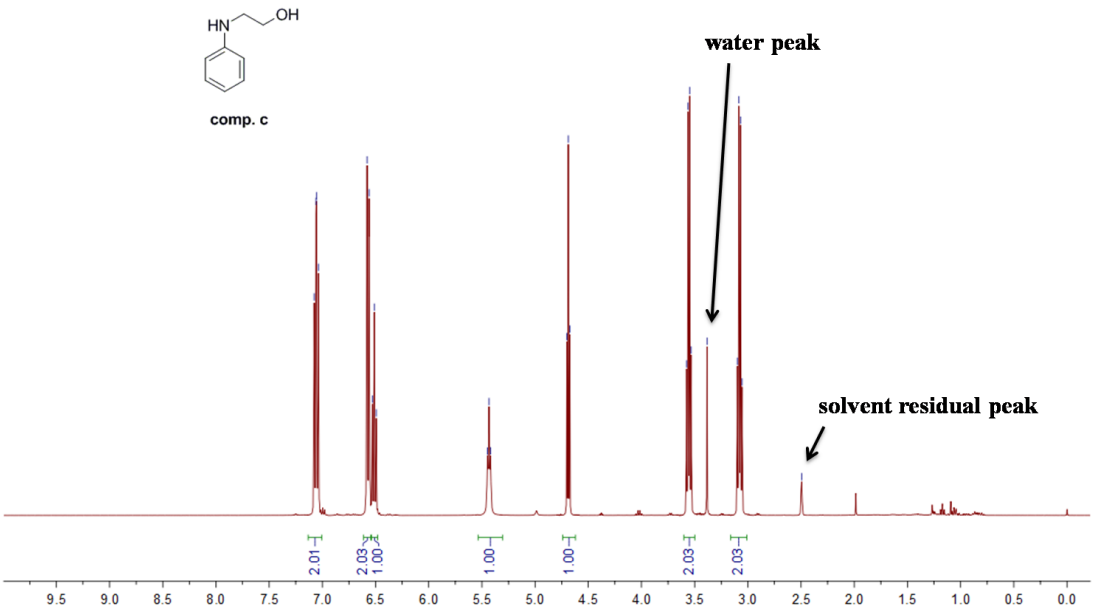

These spectral data indicated that the compounds were synthesized correctly with high purities.

Spectral copies of ^{1}H NMR of comp. b in D_2O without and with $Ca(OH)_2$

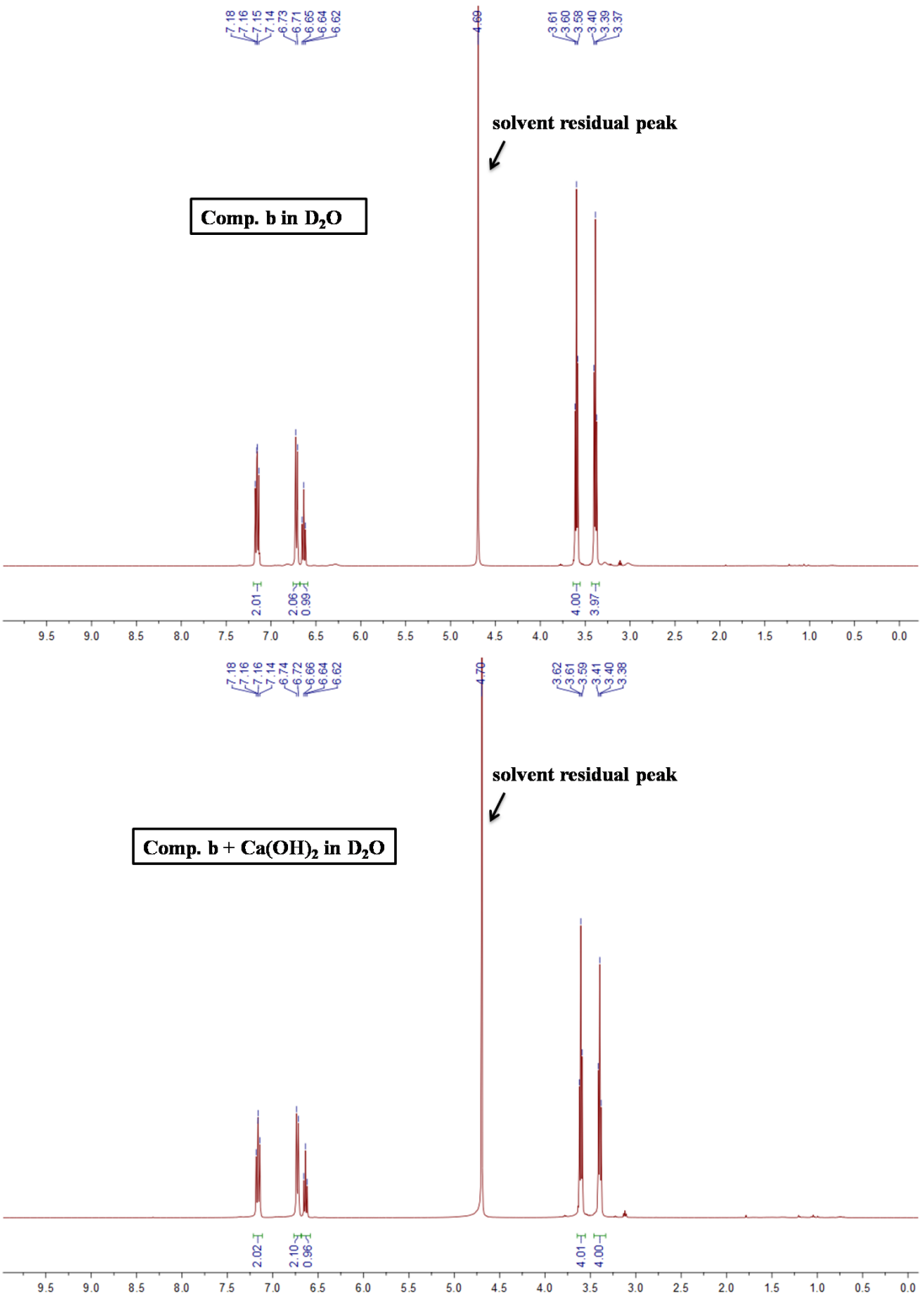

No changes of chemical shifts were detected, indicating there was no interaction between comp. b and Ca^{2+}.

Mass spectra of comp. b in water containing $Ca(OH)_2$

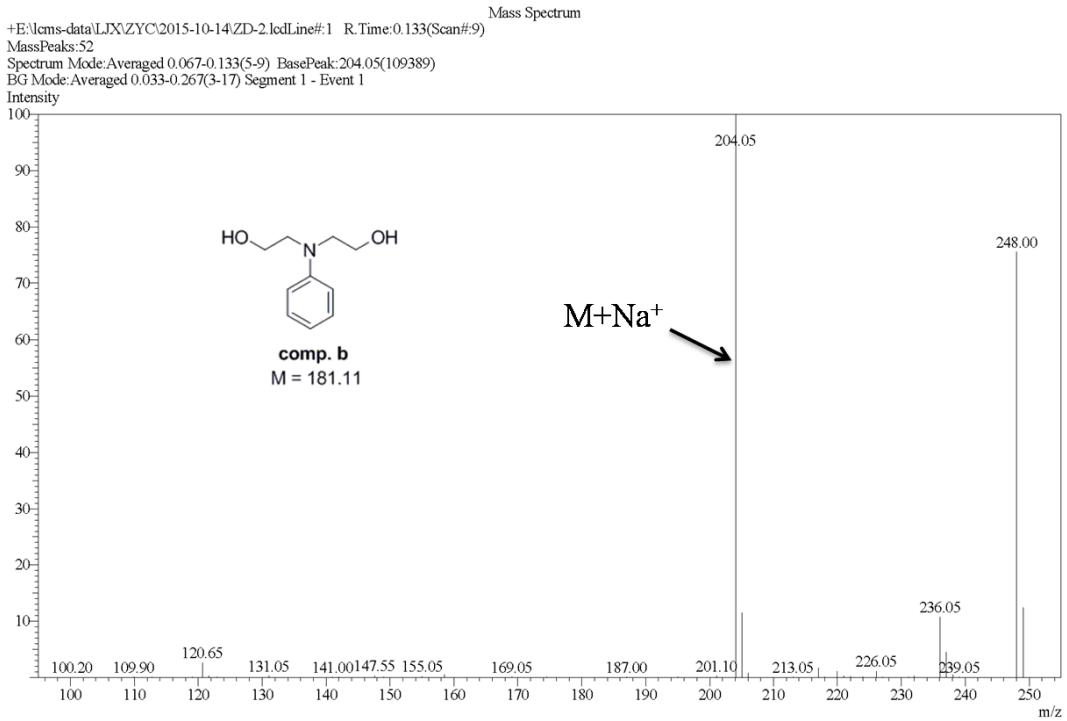

In our study, electrospray ionization mass spectrometry (ESI-MS) was used to verify the existence of comp. b-Ca^{2+} complex. The ions observed by mass spectrometry may be quasi molecular ions created by the addition of a hydrogen cation and denoted $[M + H]^+$, or of another cation such as sodium ion, $[M + Na]^+$. In the above mass spectra, the $[M+Na]^+$ molecular ion (m/z calcd for $C_{10}H_{15}NNaO_2$ $[M+Na]^+$ 204.10, found 204.05) was detected and we did not detected molecular-ion peaks of any potential comp. b-Ca^{2+} complexes, suggesting there was no comp. b-Ca^{2+} complexes in SCP solutions.

ACKNOWLEDGEMENTS

The study of this work is financially supported by National Basic Research Program of China (973 Program) (Grant No. 2015CB655105) and National Natural Science Foundation of China (NSFC) (Grant No. 51208236). The authors gratefully acknowledge their financial support.

References

1. M. Ormellese, F. Bolzoni, S. Goidanich, M. Pedeferri and A. Brenna, *Corros. Eng. Sci. Technol.*, 46 (2011) 334.
2. T. Soylev and M. Richardson, *Constr. Build. Mater.*, 22 (2008) 609.
3. H. Song, C. Lee and K. Ann, *Cem. Concr. Compos.*, 30 (2008) 113.
4. K. Ann and H. Song, *Corros. Sci.*, 49 (2007) 4113.
5. G. Batis, P. Pantazopoulou and A. Routoulas, *Cem. Concr. Compos.*, 25 (2003) 371.
6. C. Nmai, *Cem. Concr. Compos.*, 26 (2004) 199.
7. T. Soylev, C. McNally and M. Richardson, *Cem. Concr. Compos.*, 29 (2007) 357.
8. J. Kubo, Y. Tanaka, C. Page and M. Page, *Constr. Build. Mater.*, 39 (2013) 2.
9. H. Lee, H. Ryu, W. Park and M. Ismail, *Materials*, 8 (2015) 251.
10. T. Chaussadent, W. Nobel-Pujol, F. Farcas, I. Mabille and C. Fiaud, *Cem. Concr. Res.*, 36 (2006) 556.

11. T. Ostnor and H. Justnes, *Adv. Appl. Ceram.*, 110 (2011) 131.
12. M. Blankson and S. Erdem, *Constr. Build. Mater.*, 77 (2015) 59.
13. L. Yohai, M. Vazquez and M. Valcarce, *Electrochim. Acta*, 102 (2013) 88.
14. J. Hu, D. Koleva, P. Petrov and K. van Breugel, *Corros. Sci.*, 65 (2012) 414.
15. B. Bhuvaneshwari, A. Selvaraj, N. Iyer and L. Ravikumar, *Mater. Corros.*, 66 (2015) 387.
16. M. Mennucci, E. Banczek, P. Rodrigues and I. Costa, *Cem. Concr. Compos.*, 31 (2009) 418.
17. F. Fei, J. Hu, J. Wei, Q. Yu and Z. Chen, *Constr. Build. Mater.*, 70 (2014) 43.
18. X. Zhou, H. Yang and F. Wang, *Corros. Sci.*, 54 (2012) 193.
19. X. Zhou, H. Yang and F. Wang, *Electrochim. Acta*, 56 (2011) 4268.
20. J. Li, B. Zhao, J. Hu, H. Zhang, S. Dong, R. Du and C. Lin, *Int. J. Electrochem. Sci.*, 10 (2015) 956.
21. A. da Silva, E. D'Elia and J. Gomes, *Corros. Sci.*, 52 (2010) 788.
22. V. Saliyan and A. Adhikari, *Corros. Sci.*, 50 (2008) 55.
23. Z. Zhang, S. Chen, Y. Li, S. Li and L. Wang, *Corros. Sci.*, 51 (2009) 291.
24. A. Yuce, B. Mert, G. Kardas and B. Yazici, *Corros. Sci.*, 83 (2014) 310.
25. L. Mechmeche, L. Dhouibi, M. Ben Ouezdou, E. Triki and F. Zucchi, *Cem. Concr. Compos.*, 30 (2008) 167.
26. H. Zheng, W. Li, F. Ma and Q. Kong, *Constr. Build. Mater.*, 37 (2012) 36.
27. F. Wombacher, U. Maeder and B. Marazzani, *Cem. Concr. Compos.*, 26 (2004) 209.
28. A. Welle, J. Liao, K. Kaiser, M. Grunze, U. Mader and N. Blank, *Appl. Surf. Sci.*, 119 (1997) 185.
29. J. Gaidis, *Cem. Concr. Compos.*, 26 (2004) 181.
30. E. Rakanta, T. Zafeiropoulou and G. Batis, *Constr. Build. Mater.*, 44 (2013) 507.
31. J. Xu, L. Jiang and F. Xing, *Mater. Corros.*, 61 (2010) 802.
32. W. Liu, H. Cao, H. Zhang, H. Zhang, K. Chung, C. He, H. Wang, F. Kwong and A. Lei, *J. Am. Chem. Soc.*, 132 (2010) 16737.
33. M. Ormellese, L. Lazzari, S. Goidanich, G. Fumagalli and A. Brenna, *Corros. Sci.*, 51 (2009) 2959.
34. J. Cai, C. Chen, J. Liu and W. Zhou, *Int. J. Electrochem. Sci.*, 7 (2012) 10894.
35. J. Liu, C. Chen, J. Cai, J. Liu and G. Cui, *Mater. Corros.*, 64 (2013) 1075.
36. J. Cai, C. Chen and J. Liu, *Corros. Eng. Sci. Technol.*, 49 (2014) 66.
37. A. Fouda, G. Elewady, K. Shalabi and H. El-Aziz, *RSC Adv.*, 5 (2015) 36957.
38. M. Ormellese, F. Bolzoni, L. Lazzari, A. Brenna and M. Pedeferri, *Mater. Corros.*, 62 (2011) 170.
39. O. Exner, *J. Phys. Org. Chem.*, 12 (1999) 265.
40. L. Valek, S. Martinez, D. Mikulić and I. Brnardić, *Corros. Sci.*, 50 (2008) 2705.
41. F. Bentiss, M. Traisnel and M. Lagrenee, *Corros. Sci.*, 42 (2000) 127.
42. H. Jamil, M. Montemor, R. Boulif, A. Shriri and M. Ferreira, *Electrochim. Acta*, 48 (2003) 3509.
43. H. Zheng, W. Ma and Q. Kong, *Cem. Concr. Res.*, 55 (2014) 102.
44. M. Lebrini, M. Lagrenée, H. Vezin, M. Traisnel and F. Bentiss, *Corros. Sci.*, 49 (2007) 2254.
45. M. Morad, *J. Appl. Electrochem.*, 38 (2008) 1509.
46. M. Bouklah, B. Hammouti, M. Lagrenée and F. Bentiss, *Corros. Sci.*, 48 (2006) 2831.
47. Y. Yang, S. Bae and Y. Hwang, *Tetrahedron Lett.*, 54 (2013) 1239.